REPORT DOCUMENTATION PAGE

1a REPORT SECURITY CLASSIFICATION: Unclassied	1b RESTRICTIVE MARKINGS
2a SECURITY CLASSIFICATION AUTHORITY	3 DISTRIBUTION / AVAILABILITY OF REPORT: Approved for public release; Distribution unlimited
2b DECLASSIFICATION / DOWNGRADING SCHEDULE	
4 PERFORMING ORGANIZATION REPORT NUMBER(S)	5 MONITORING ORGANIZATION REPORT NUMBER(S): AFOSR-TR- 88-0830
6a NAME OF PERFORMING ORGANIZATION: Carnegie Mellon University; 6b OFFICE SYMBOL (If applicable)	7a NAME OF MONITORING ORGANIZATION: AFOSR
6c ADDRESS (City, State, and ZIP Code): 4400 Fifth Avenue, Pgh., PA 15213	7b ADDRESS (City, State, and ZIP Code): Bldg. 410, Bolling AFB, D.C. 20332-6448
8a NAME OF FUNDING / SPONSORING ORGANIZATION: AFOSR; 8b OFFICE SYMBOL (If applicable): NC	9 PROCUREMENT INSTRUMENT IDENTIFICATION NUMBER: F49620-85-C-1040
8c ADDRESS (City, State, and ZIP Code): Bldg. 410, Bolling AFB, D. C. 20332-6448	10 SOURCE OF FUNDING NUMBERS: PROGRAM ELEMENT NO 61102F; PROJECT NO 2303; TASK NO A3; WORK UNIT ACCESSION NO

11 TITLE (Include Security Classification)
Rheological, Rheo-Optical and Light Scattering Studies on Nematic Solutions of Poly(1,4-Phenylene-2,6-Benzobisthiazole)

12 PERSONAL AUTHOR(S)
G. C. Berry

13a TYPE OF REPORT	13b TIME COVERED	14 DATE OF REPORT (Year, Month, Day)	15 PAGE COUNT
Preprint Report	FROM _____ TO _____	1988	

16 SUPPLEMENTARY NOTATION
MARCEL DEKKER, Inc New York and Basel

17 COSATI CODES			18 SUBJECT TERMS (Continue on reverse if necessary and identify by block number)
FIELD	GROUP	SUB-GROUP	

19 ABSTRACT (Continue on reverse if necessary and identify by block number)

Rheological and rheo-optical properties of mesogenic solutions of rodlike polymers are discussed. Some of the salient features of the observed behavior with isotropic solutions described, including a single-integral constitutive equation that is found to be useful, and a review of certain aspects of theoretical treatments of the viscosity of nematic fluids. The light scattering experiments are discussed, including studies on a monodomain formed with a PBT solution. Aspects of the rheological behavior of nematic solutions of PBT are considered, first for recently small strain and then for deformation with large strain rates.

20 DISTRIBUTION / AVAILABILITY OF ABSTRACT	21 ABSTRACT SECURITY CLASSIFICATION	
☐ UNCLASSIFIED/UNLIMITED ☒ SAME AS RPT ☐ DTIC USERS	Unclassified	
22a NAME OF RESPONSIBLE INDIVIDUAL: ~~Cap C. Berry~~ Lary Davis USAF	22b TELEPHONE (Include Area Code): (~~412~~) ~~268-31~~ 202 767-4960	22c OFFICE SYMBOL: NC

DD FORM 1473, 84 MAR — 83 APR edition may be used until exhausted. All other editions are obsolete.

SECURITY CLASSIFICATION OF THIS PAGE
UNCLASSIFIED

HIGH MODULUS POLYMERS

Approaches to Design and Development

edited by

Anagnostis E. Zachariades
IBM Almaden Research Center
San Jose, California

Roger S. Porter
Department of Polymer Science and Engineering
University of Massachusetts
Amherst, Massachusetts

MARCEL DEKKER, INC. New York and Basel

7

RHEOLOGICAL, RHEO-OPTICAL AND LIGHT SCATTERING STUDIES ON NEMATIC SOLUTIONS OF POLY(1,4-PHENYLENE-2,6-BENZOBISTHIAZOLE)

Guy C. Berry, Kazunori Se and Mohan Srinivasarao

INTRODUCTION

Rheological and rheo-optical properties of mesogenic solutions of rodlike polymers are discussed in the following. In the remainder of this section, some of the salient features of the observed behavior with isotropic solutions will be described, including a single-integral constitutive equation that is found to be useful, and a review of certain aspects of theoretical treatments of the viscosity of nematic fluids. The light scattering experiments are discussed in the next section, including studies on a monodomain formed with a PBT solution. In the final two sections, aspects of the rheological behavior of nematic solutions of PBT are considered, first for recently small strain and then for deformation with large strain rates.

Isotropic Solutions

Important rheological properties of isotropic solutions of the rodlike polymers poly(1,4-phenylene-2,6-benzobisthiazole), PBT, and poly(1,4-phenylene terephthalamide), PPTA, can be represented by a single-integral constitutive equation of the BKZ type [1-5]. With this relation, the components $\sigma_{\alpha\beta}(t)$ of the stress tensor are given by

$$\sigma_{\alpha\beta}(t) = -\int_0^\infty ds \ \frac{\partial G_0(s)}{\partial s} \ Q_{\alpha\beta}(t, t-s) \ . \tag{1}$$

Here $G_0(t)$ is the shear relaxation modulus determined in a linear viscoelastic response [6] and $Q_{\alpha\beta}$ depends only on the strain-history. Expressions of $Q_{\alpha\beta}$ for shear deformation and uniaxial elongation are available [5]. For recently small deformations, $Q_{\alpha\beta}$ reduces to $Q^0_{\alpha\beta}$ of linear viscoelasticity. For example, for a shear deformation, $Q^0{}_{12}(t_1, t_2) = \gamma(t_1, t_2) = \gamma(t_1) - \gamma(t_2)$, where $\gamma(t)$ is the shear strain at time t [6]. With this deformation, nonlinear effects can be represented by [2,4,6,7]

$$Q_{12}(t_1, t_2) = \gamma(t_1, t_2) F_s[\gamma(t_1, t_2)] \ . \tag{2}$$

The nonlinear strain-measure is approximately given by [2,7]

$$F_s(\gamma) \approx \exp[-m(|\gamma| - \gamma')/\gamma''] \tag{3}$$

where m is zero for $|\gamma| < \gamma'$ and unity otherwise. Application of these relations to give the dependence on shear rate κ of the steady-state viscosity η_κ, the recoverable compliance R_κ obtained after steady flow, and the first-normal stress function $N_\kappa(1)$ are discussed elsewhere [2,7]. (Here $R_\kappa = \gamma_R/\kappa\eta_\kappa$ with γ_R the recoverable strain, and $N_\kappa(1) = \nu^{(1)}/2(\kappa\eta_\kappa)^2$ with $\nu^{(1)}$ the first-normal stress difference). In particular, with $G_0(t)$ in the form

$$G_0(t) = \Sigma\eta_i\tau_i^{-1} \exp(-t/\tau_i) \tag{4}$$

these relations may be integrated to give η_κ, R_κ and $N_\kappa^{(1)}$ in the forms [7]

$$\eta_\kappa = \Sigma\eta_i[1 - q(\beta\gamma''\kappa/\tau_i)] \tag{5}$$

$$\eta_0\eta_\kappa R_\kappa \approx \Sigma\eta_i\tau_i[1 - q(\beta\gamma''\kappa/\tau_i) \exp(-\eta_\kappa R_\kappa/\tau_i)] \tag{6}$$

$$\eta_\kappa^2 N_\kappa^{(1)} = \Sigma\eta_i\tau_i[1 - p(\beta\gamma''\kappa/\tau_i)] \ . \tag{7}$$

The functions q, p and β are given elsewhere [2]; $\beta \approx 1$, is a weak function of γ'/γ''. Study of the linear viscoelastic behavior can give the η_i, τ_i parameters [6]. The flow birefringence $\Delta n^{(13)}$ in the [1-3] flow plane (*i e*, shear gradient in direction-2 with flow in direction-1) has been represented in terms of the preceding by use of the stress-optic law [1]:

$$M_\kappa = \Delta n^{(13)}/(\kappa\eta_\kappa)^2 = 2C' N_\kappa^{(1)} \tag{8}$$

with C' a constant equal to the limiting value of $M_\kappa/2R_\kappa$ for small κ.

The same constitutive equation may be used [2,3] to determine the stress relaxation function $\hat{\eta}_\kappa(t)$ and the flow birefringence relaxation $\hat{M}_\kappa(t)$, each determined following cessation of steady flow at shear rate κ ($\hat{\eta}_\kappa(t) = \sigma(t)/\kappa$ and $\hat{M}_\kappa(t) = \Delta n^{(13)}(t)/(\kappa\eta_\kappa)^2$ where $\sigma(t)$ and $\Delta n^{(13)}(t)$ are, respectively, the stress and birefringence at time t after cessation of flow). Thus,

$$\hat{\eta}_\kappa(t) = \Sigma\eta_i[1 - q(\beta\gamma''\kappa/\tau_i)] \exp(-t/\tau_i) \tag{9}$$

and $\hat{M}_\kappa(t) = 2C'\hat{N}_\kappa^{(1)}(t)$, with

$$\eta_\kappa^2\hat{N}_\kappa^{(1)}(t) = \Sigma\eta_i\tau_i[1 - p(\beta\gamma''\kappa/\tau_i)] \exp(-t/\tau_i) \ . \tag{10}$$

A theoretical estimate [8] of η_0 for isotropic solutions of rodlike chains given by the relation

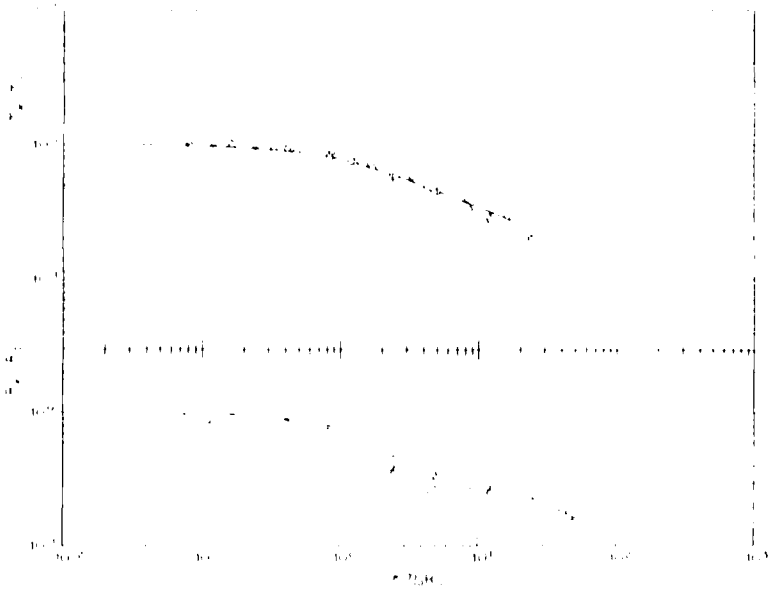

Figure 1. Rheological data for isotropic (-0, 0) and nematic (0-, 0) solutions of PBT-53 (0.0323 weight fraction) polymer. With the latter, η_0 is replaced by η_p, see text. The curves are calculated with Eq. (5) and (6) using experimentally determined values of τ_1 and η_1 (From reference 3).

$$\eta_0 = \eta_0^{ISO}(1 - B\,cL/\alpha M_L)^{-2} \tag{11a}$$

$$\eta_0^{ISO} = KN_A^2M[\eta]\eta_s(cL/M_L)^3 \tag{11b}$$

provides a satisfactory representation of experimental data [1,2]. Here, M, $[\eta]$ and L are the molecular weight, intrinsic viscosity and length, respectively, of the chain, $M_L = M/L$, c is the concentration (wt/vol), η_s is the solvent viscosity, α is the value of cL/M_L for onset of the nematic state, B is a constant near unity, and K is a constant (ca. 1.5×10^{-4} in cgs units) [2].

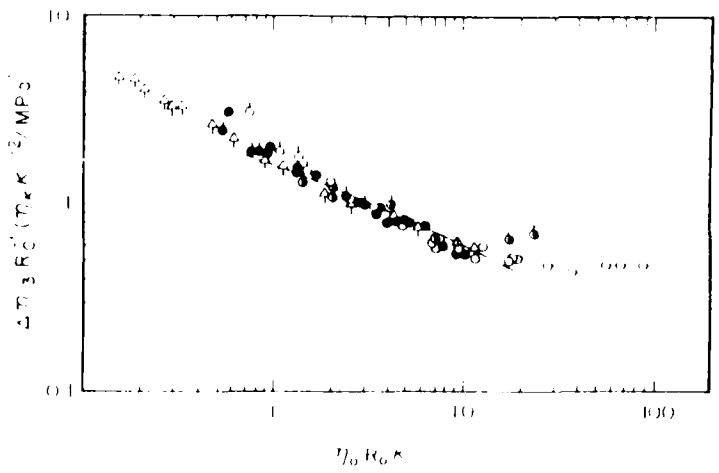

Figure 2. The steady-state flow birefringence *versus* the reduced shear rate $\eta_0 R_0 \kappa$ for an isotropic solution of PBT (0.0255 weight fraction) at several temperatures. The curve is calculated with Eq. (7) and (8) using experimentally determined values of τ_1 and η_1 (from reference 2).

In many cases, the parameter

$$\tau_c = \eta_0 R_0 = \lim_{\kappa=0} \eta_\kappa R_\kappa \tag{12}$$

is useful in reducing data over a range of temperature or concentration [1,2,7]. Typical data on η_κ/η_0, R_κ/R_0 and M_κ/M_0 *versus* $\tau_c\kappa$ for an isotropic solution of PBT [2] are shown in Figs. 1 and 2. The representation of the experimental curves by Eqs. (5-8) is satisfactory, provided the experimental $G_0(t)$ is used. The latter decays more slowly than a theoretical estimate according to Doi and Edwards [5]. Typical data on $\hat{\eta}_\kappa(t)/\eta_\kappa$ and $\hat{M}_\kappa(t)/M_\kappa$ *versus* t/β_κ for isotropic solutions of PBT [2] are shown in Fig. 3. Here, β_κ is an empirical parameter, about equal to $\eta_\kappa R_\kappa$.

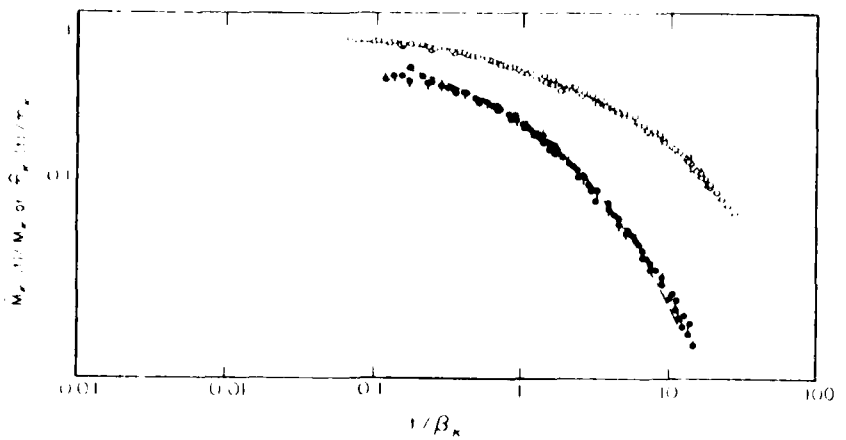

Figure 3. The reduced flow birefringence relaxation function $M_\kappa(t)/M_\kappa$ (open circles) and stress relaxation function $\hat{\eta}_\kappa(t)/\eta_\kappa$ (filled circles) for an isotropic solution of PBT (0.0294 weight fraction) for several shear rates. With $\beta_\kappa \approx \tau_\kappa R_\kappa$ (From reference 2).

Nematic Solutions

With nematic solutions of rodlike polymers, it can be anticipated that much of the preceding will not be valid owing to the long orientational coherence lengths of the nematic state. For example, since an isotropic fluid has no inherently preferred direction, the properties described by Eq. (1) do not depend on the flow direction. By contrast, under certain circumstances the rheological properties of a nematic fluid may depend markedly on the orientation of the director $\underset{\sim}{n}$; for the solutions of interest here, this may be assumed to be coincidental with the orientation of the rodlike chains. According to the Leslie-Ericksen constitutive equation [9], the viscometric properties of such a fluid may be represented in terms of six viscosity coefficients α_i ($i = 1$-6). A well-known example of this behavior is demonstrated by the viscosities η_a, η_b, and η_c calculated as σ_{12}/κ

for recently small deformations with $\underset{\sim}{n}$ fixed by an external field (*e.g.*, a magnetic field) with, respectively, $\underset{\sim}{n}$ parallel to the velocity gradient, $\underset{\sim}{n}$ parallel to the flow direction, and $\underset{\sim}{n}$ perpendicular to both the flow and the velocity gradient (*i.e.*, the Miesowicz viscosities) [10]. According to the Leslie-Ericksen constitutive equation [9], these viscosities are given by

$$\eta_a = (-\alpha_2 + \alpha_4 + \alpha_5)/2 = \eta_c + (\alpha_5 - \alpha_2)/2 \tag{13}$$

$$\eta_b = (\alpha_3 + \alpha_4 + \alpha_6)/2 = \eta_a + \alpha_3 + \alpha_2 \tag{14}$$

$$\eta_c = \alpha_4/2 \ . \tag{15}$$

Here, use is made of Parodi's relation: $\alpha_6 = \alpha_2 + \alpha_3 + \alpha_5$ [11]. The α_i coefficients also appear in the viscosity parameters occurring in the analysis of light scattering data discussed below. For example, a viscosity η_T associated with twist of the director field (without deformation of the sample) is given by [12-14]

$$\eta_T = \alpha_3 - \alpha_2 \ . \tag{16}$$

Frequently, $-\alpha_2 > |\alpha_3|$ [13], in which case η_T is close to the quantity

$$\eta_{ab} = \eta_a - \eta_b = -(\alpha_2 + \alpha_3) \ . \tag{17}$$

Additional viscosities η_B and η_S associated, respectively, with bend and splay of the director field are given by [12-14]

$$\eta_B = \eta_T - \frac{(\eta_T + \eta_{ab})^2}{4\eta_a} \tag{18}$$

$$\eta_S = \eta_T - \frac{(\eta_T - \eta_{ab})^2}{4\eta_b} \ . \tag{19}$$

If $\eta_T \approx \eta_{ab}$, then $\eta_S \approx \eta_T$ and $\eta_B < \eta_T$, as has been observed for low molecular weight nematic fluids [12].

If there are no constraints to maintain a preferred orientation of n, then the steady-state shear viscosity η_0 for recently small deformation is given by [9]

$$\eta_0 = \eta_b + \frac{1}{2}(\eta_{ab} - \eta_T)\left\{1 + \frac{\alpha_1(\eta_{ab} + \eta_T)}{4\eta_{ab}^2}\right\} \quad (20)$$

In this flow, the director orients at an angle θ_0 to the flow direction (in the shear plane), with

$$2\theta_0 = \arccos(\eta_T/\eta_{ab}) \quad (21)$$

Stable shearing flow requires $\eta_T < \eta_{ab}$; if $\eta_{ab} \approx \eta_T$, then $\eta_0 \approx \eta_b$. Finally, in elongational flow (with no constraints on the director), the elongational viscosity η_0 is given by [15]

$$\eta_0 = 3\eta_b + (\eta_{ab} - \eta_T) + \eta_d \quad (22)$$

where $2\eta_d = \alpha_5 - \alpha_2 + 2\alpha_1$. If η_d and $\eta_{ab} - \eta_T$ are much less than $3\eta_b$, then $\eta_0 \approx 3\eta_b$.

With many nematic fluids, it is possible to create a preferred direction in a sample confined between two surfaces by adsorption on the surfaces in a preferred direction [13]. The long orientational coherence of the nematic then provides the globally preferred direction. In this situation, if one plate is moved parallel to the other with velocity V, the deformation is expected to result in orientation at the angle θ_0 at distances far from the surface, but near the surfaces the orientation remains that of the adsorbed layer [9,16]. Currie and coworkers [16] have used the Leslie-Ericksen constitutive equation to compute the viscosity as a function of $\kappa = V/h$ for a number of geometries in terms of the Ericksen number E_3 defined as

$$E_3 = \sigma(V/\kappa)^2/K_3 \quad (23)$$

where σ and κ are the shear stress and shear rate, respectively, at a position with deformation at velocity V, and K_3 is the bend free

energy coefficient. For simple shear flow, V/κ is equal to the separation h of the two parallel surfaces. With this treatment, the boundary layer with thickness δ and the orientation of the adsorbed layer decreases with increasing $\kappa = V/h$, and the apparent viscosity $\eta_\delta = \sigma h/V$ is given by [16]

$$\eta_\delta = \eta_0\{1 + E^{-1/2}\Pi_\delta(\theta_2, \theta_1, \theta_0)\}^{-1} \quad (24)$$

where η_0 is given by Eq. (20), with θ_1 and θ_2 the orientation angles (in the plane of shear) between the flow direction and the direction of $\underset{\sim}{n}$ for the adsorbed layers at the two surfaces, and Π_δ depends on the viscosity coefficients α_i. Questions of flow stability have been explored within the frame of this model [9,16]. With Eq. (24), η_δ decreases toward η_0 with decreasing κ as the shear rate is increased, until the boundary layer is negligibly thin. For small κ, η_δ increases toward a limiting value specified by θ_1, θ_2 and the viscosity coefficients.

Theoretical treatments for a nematic *fluid comprising long* rodlike macromolecules have given estimates for the viscosity coefficients α_i in terms of the order parameter S characterizing the nematic fluid [15,17,18]; S is expected to increase with increasing cl.. Values of $\alpha_i/\eta_0^{[SO}(1 - S)^2$ for two such treatments [17-18] are given in Table 1. (For these treatments $\alpha_6 = \alpha_5 + \alpha_2 + \alpha_3$ so that only five of the six coefficients are independent). The principal difference between the two

Table 1. Leslie-Ericksen Coefficients for Rodlike Polymers

Parameter[a]	Reference 18	Reference 17[b]
α_1/k	$-S^2$	$-rS^2$
α_2/k	$-S(1+2S)/(2+S)$	$-(S/2)[3(r-1)+2(1+2S)]/[3(r-1)+2+S] = -S(4S-1)/(5S-2)$
α_3/k	$-S(1-S)/(2+S)$	$-(S/2)[3(r-1)+2(1-S)]/[3(r-1)+2+S] = S(1-S)/(5S-2)$
α_4/k	$(1-S)/3$	$(7-5S-2rS^2)/35 = (1-S)[1-(2/35)(1-S)(7+4S)]/3$
α_5/k	S	$S(5+2rS)/7 = S[1-(2/21)(1-S)(3-4S)]$
α_6/k	0	$-2S(1-rS)/7 = -2S(1-S)(3+4S)/21$
λ^{SC}	$1-(1-S)/3$	$r-(1-S)/3 = -1-5(1-S)/3$
r		$1-4(1-S)/3$

treatments is in the estimate for α_3, which is different in sign for the two treatments. This difference is critical as it affects the sign of $\eta_{ab} - \eta_T$, which must be positive for stable flow. Thus, for the treatment in reference 18, $\eta_T < \eta_{ab}$ and shear flow is predicted to be stable, with

$$\eta_0 = \eta_b \frac{(1 + 2S)(2 + 3S)}{(2 + S)} \tag{25}$$

$$\eta_b = \eta_0^{ISO} \frac{(1 - S)^4}{(1 + S/2)} \tag{26}$$

where η_0^{ISO} is given by Eq. (11b). For the treatment in reference 15, $\eta_T > \eta_{ab}$, and shear flow is predicted to be unstable. For the latter treatment,

$$\eta_b = \eta_0^{ISO} \frac{2(1 - S)^4}{21} \{4(4S + 7) + 35(5S - 2)^{-1}\} \tag{27}$$

which is larger than η_b given by Eq. (26) for the same S. According to Eqs. (25-26), η_0 is expected to decrease as cL/M_L exceeds α, through both of the factors $(1\text{-}S)^4$ and $(1\text{-}B)^2$:

$$\frac{\eta_0}{(\eta_0)_{max}} = (cL/M_L\alpha)^3(1\text{-}S)^4(1\text{-}B)^2 f(S) \tag{28}$$

where $f(S) \approx 10/(1+2S)$ and $(\eta_0)_{max}$ is the value of η_0 given by Eq. (11a) with $cL/M_L\alpha = 1$. Behavior similar to this has been reported [3], provided viscometric data are interpreted in a particular way (see below).

a) $k = k'\eta_0^{ISO}(1 - S)^2$; η_0^{ISO} given by Eq. (11b) and k' is 10 in reference 17 or 6 in reference 18 (The factor k' was omitted in reference 24). Since $\alpha_2 + \alpha_3 = \alpha_6 - \alpha_5$, only five of the α_i are independent.

b) Based on asymptotic behavior for α_1 given in reference 17 and approximate relations for λ and r [24].

c) $\lambda = \eta_{ab}/\eta_T$, see Eqs. (16) and (17).

LIGHT SCATTERING STUDIES OF LIQUID CRYSTALLINE PBT SOLUTIONS

Solutions of PBT (or PPTA) of a suitable concentration undergo a phase transformation from an isotropic to a nematic solution with decreasing temperature, passing through a biphasic region for a narrow temperature range [1-3]. Data on the Rayleigh ratios $R_{HV}(\theta)$ and $R_{VV}(\theta)$ determined through such a transformation are shown in Fig. 4 for scattering with $\theta = 20°$. Here the symbols Hv and Vv denote the horizontally and vertically polarized components of the scattering with vertically polarized light, respectively. Details of this experiment will be published elsewhere [20]. A solution of PBT ($M_w = 3.4 \times 10^4$) in methane sulfonic acid (weight fraction w of the polymer equal to 0.041) was placed between parallel glass plates. The assembly was sealed to prevent contamination by atmospheric moisture. As shown in Fig. 4, both $R_{HV}(20)$ and $R_{VV}(20)$ increase with decreasing T as the sample is cooled ($dT/dt \approx -0.003$K/s), with the ratio $R_{HV}(20) / R_{VV}(20)$ increasing from about 0.02 at 110°C to 0.9 for T<70°C.

Immediately after being cooled to 25°C, the sample exhibited a mottled texture with transmission, $T_\perp$ and $T_\parallel$ between either crossed or parallel polars respectively, being low (<4%). Upon annealing at 25°C, both $R_{VV}(20)$ and $R_{HV}(20)$ decreased, with the ratio $R_{HV}(20)/R_{VV}(20)$ remaining nearly unchanged. The scattered intensity decreased exponentially on annealing, with a time constant of about 100 hrs. After annealing, the sample exhibited a smooth texture when viewed between parallel or crossed polars, with the exception of a few large, looping disclinations, see Fig. 5. When viewed between crossed polars, the sample exhibited a blotchy pattern of extinction that varied as the sample was rotated between the crossed polars; in some areas extinction never obtained. This appearance is attributed to smooth variations of the director orientation throughout the fluid; the rodlike chains tend to be parallel, with a preferred orientation, but that orientation varies smoothly throughout the sample. Adsorption of the polymer on the glass surfaces could serve to stabilize such a texture.

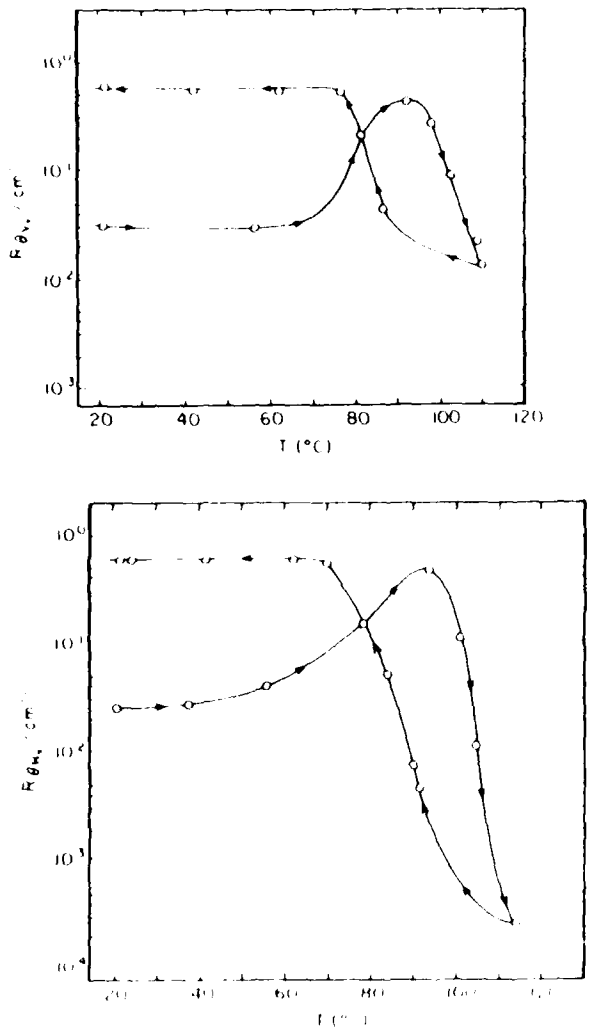

Figure 4. The Rayleigh scattering ratio (20 deg scattering angle) determined as a function of temperature for a nematic solution of PBT (0.041 weight fraction). The thermal history is indicated by the arrowheads; the temperature was changed continuously over the range 20 to 110 to 20°C over 16 hr. The symbols H_v and V_v designate, respectively, the horizontally and vertically polarized components of the scattering with vertically polarized incident light.

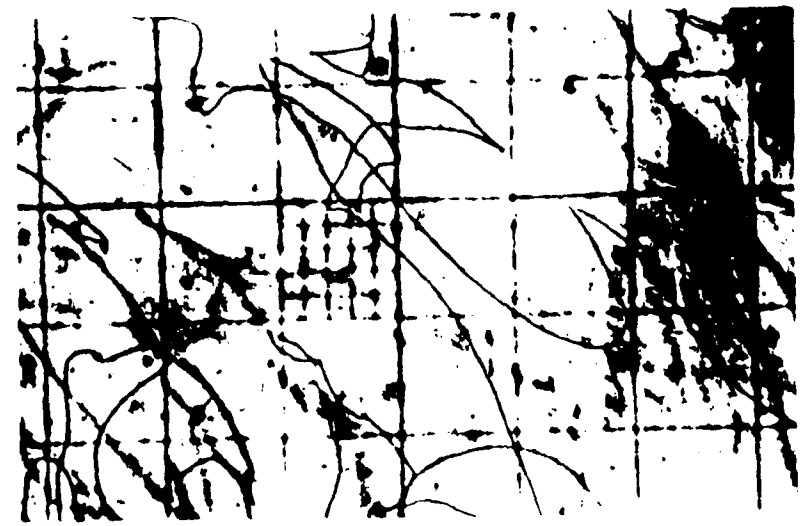

Figure 5. Photomicrograph of a nematic solution viewed between crossed polars. Except for a few disclinations, the texture is smooth, but not uniformly oriented. The disclinations are found only near the bounding surfaces, *e g* , the disclinations near the upper surface are in sharp focus and those at the opposite surface appear diffuse. The larger grid has a 220 μm spacing.

As shown in Fig. 4, both $R_{VV}(20)$ and $R_{HV}(20)$ passed through a maximum with increasing temperatures when the annealed specimen was reheated ($dT/dq \approx 0.003K/s$), with the maximum scattering occurring near the temperature (92°C) for the onset of a biphasic state visible by polarized microscopy. As the temperature exceeded 60°C, the smooth texture was replaced by an increasingly complex texture and increased scattering.

Photon correlation data were obtained for the sample with smooth texture with both the VV and HV scattering, giving $G^{(2)}_{VV}(\tau)$ and $G^{(2)}_{HV}(\tau)$ intensity correlation functions, respectively. In both cases the correlation function, decayed over a wide range of time, *e g* , with the representation

$$G^{(2)}(\tau)/G^{(2)}(\infty) = 1 - f(A)\{\Sigma\, r_i \exp - \gamma_i \tau\}^2 \qquad (29)$$

the distribution of the coherence times γ_i^{-1} spanned from 0.1 to 10^3 ms. (Here, f(A) is an instrumental coherence factor equal to $[G^{(2)}(0) - G^{(2)}(\infty)]/G^{(2)}(\infty)$, and $\Sigma\, r_i = 1$).

A monodomain sample better suited for light scattering studies was prepared by slow extrusion of the sample into a rectangular channel (cell dimensions: 0.03 cm thick, 1 cm wide and 1.5 cm along the flow direction). It was reasoned that this procedure would cause a preferential orientation (along the flow direction) of the polymer adsorbed on the glass surfaces, resulting in a globally preferred orientation throughout the solution at equilibrium. Shortly after cessation of flow, the sample exhibited strong birefringence, with a preferred orientation in the flow direction, and scattered light very strongly. In addition, the sample exhibited several nonbirefringent narrow bands precisely perpendicular to the flow direction. As the sample aged, these bands were converted to large loop disclinations going completely around the sample in a plane normal to the former flow direction. These features may be related to flow instabilities related to complete rotation of the director in the shear plane, so that the orientation is nearly homeotropic in the center of the narrow, nonbirefringent bands (see below). Several hours subsequent to cessation of flow, the fluid developed strong birefringence, which extinguished between crossed polars for cell orientation with the cell axis (the flow direction during the extrusion) parallel to the axis of either the polarizer or the analyzer. At this stage, a dense field of disclinations obtained near either surface, but the interior was free of such defects. After several days, almost all of the disclinations disappeared, leaving a few loop disclinations at the surfaces, with a sharpened extinction between crossed polars, see Fig. 6. The solution was also dichroic, with preferred directions parallel and perpendicular to the cell axis (maximum extinction for light polarized along the cell axis). For wavelengths near the absorption maximum (440 nm) the extraordinary ray is completely extinguished, and the sample performed as a polarizer. Viewed in natural light, the solution appeared transparent (yellow in color), being nearly featureless.

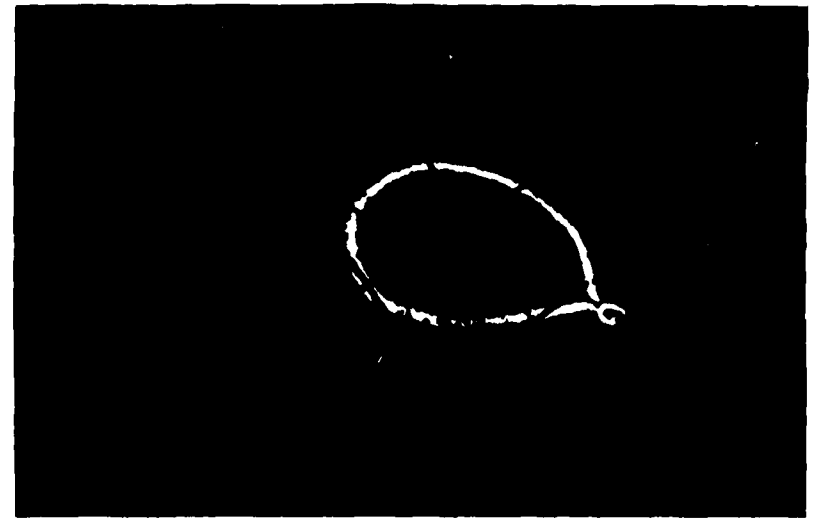

Figure 6. Photomicrograph of an oriented nematic solution of PBT obtained between cross polars. The sample orientation of the nematic being parallel to the polarizer. The loop disclination shown in the micrograph gradually shrank, and disappeared after several weeks. The larger grid has an 80 μm spacing.

For a liquid crystal monodomain, the Rayleigh ratio depends on the orientation of the director relative to the plane containing the incident and scattered rays, the polarization of these, and the scattering angle θ. Thus, the Rayleigh ratio may be expressed in the form [12-14].

$$R_{\underset{\sim}{A},\,\underset{\sim}{P},\,\underset{\sim}{n}}(q_\perp, q_\parallel) \propto (n_e - n_0)^2 \sum_{\alpha=1,2} \Gamma_\alpha \qquad (30a)$$

$$\Gamma_\alpha = F_\alpha(\underset{\sim}{P}, \underset{\sim}{A}, \underset{\sim}{n})/\hat{K}_\alpha(q_\perp, q_\parallel) \qquad (30b)$$

where $\underset{\sim}{P}$, $\underset{\sim}{A}$ and $\underset{\sim}{n}$ designate the unit vectors defining the orientation of the polarizer, analyzer and director, respectively, with respect to the scattering plane containing the incident ray,

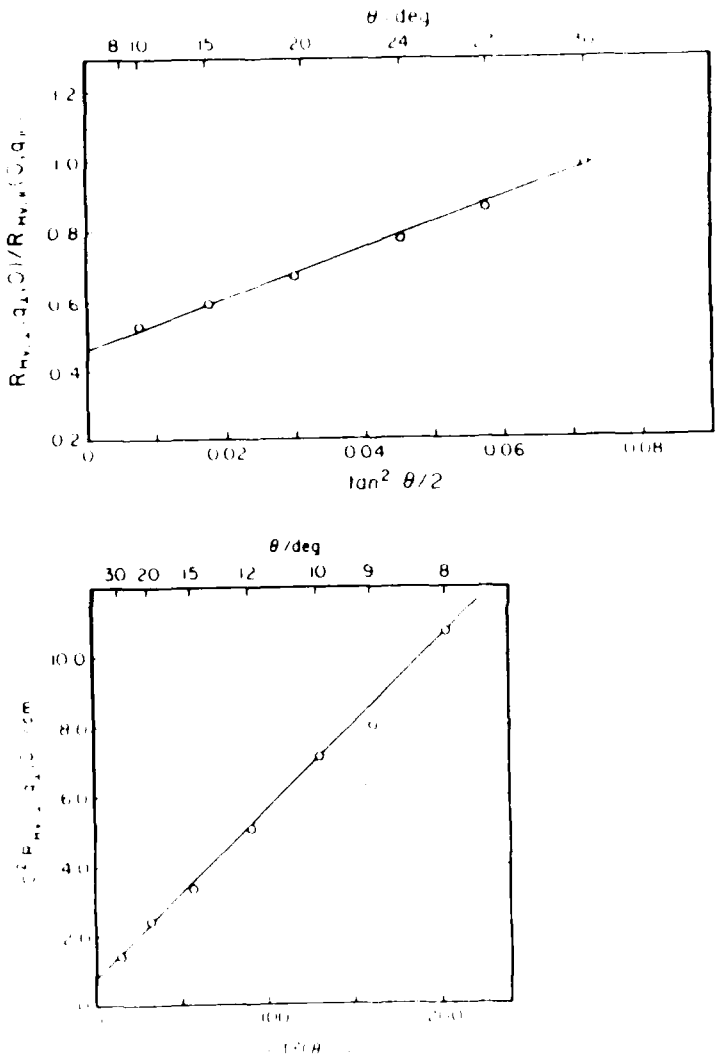

Figure 7. Plots of the scattering determined with an oriented monodomain solution of PBT (0.0411 weight fraction). The upper and lower parts correspond to plots according to Eqs. (34) and (35), respectively.

the scattered ray and the scattering vector $\underset{\sim}{q}$. In Eq. (30), $F_a(\underset{\sim}{P}, \underset{\sim}{A}, \underset{\sim}{n})$ depends only on the geometrical arrangement used in the scattering experiment, and $\hat{K}_a$ depends on the Frank free energy coefficients $K_1 = K_S$, $K_2 = K_T$ and $K_3 = K_B$ for splay, twist and bend deformations of the director field, respectively, through the expression

$$\hat{K}_a(q_\perp, q_\parallel) = K_a q_\perp^2 + K_3 q_\parallel^2 \tag{31}$$

$$q_\parallel = (\underset{\sim}{q} \cdot \underset{\sim}{n}) \tag{32}$$

$$q_\perp = (q^2 \quad q_\parallel^2)^{1/2} \tag{33}$$

For example, for the horizontal component of the scattering obtained with vertically polarized incident light,

$$\frac{R_{HV,\perp}(q_\perp, 0)}{R_{HV,\parallel}(0, q_\parallel)} = \frac{K_B}{K_S} + \frac{K_B}{K_T} \tan^2 \frac{\theta}{2} \tag{34}$$

where the subscripts $_\perp$ and $_\parallel$ designate the director orientation perpendicular and parallel to the scattering plane, respectively. In another arrangement with the vertical component of the scattering obtained with horizontally polarized incident light,

$$R_{VH,\parallel}(q_\perp, 0) \propto \frac{(n_e - n_0)^2}{K_T} \left(1 + \frac{K_T}{K_S} \cot^2 \frac{\theta}{2}\right) \tag{35}$$

Data, obtained according to these two cases for the PBT solution studied, are shown in Fig. 7.

The dynamic scattering depends on the elastic constants along with the viscosities for twist, bend and splay:

$$G^{(2)}_{\underset{\sim}{A},\underset{\sim}{P},\underset{\sim}{n}}(q_\perp, q_\parallel; \tau) - G^{(2)}_{\underset{\sim}{A},\underset{\sim}{P},\underset{\sim}{n}}(q_\perp, q_\parallel; 0) + f\{\sum_{a=1,2} \Gamma_a \exp[-\tau/\tau_a(q_\perp, q_\parallel)]\}^2 \tag{36a}$$

where

$$\tau_a(q_\perp, q_\parallel) = \hat{\eta}_a(q_\perp, q_\parallel)/\hat{K}_a(q_\perp, q_\parallel) \tag{36b}$$

and Γ_a is given by Eq. (30b). The function $\hat{\eta}_a(q_\perp, q_\parallel)$ is complex, but simplifies for special values of $q_\perp$ and $q_\parallel$:

$$\hat{\eta}_1(0, q_\parallel) = \hat{\eta}_2(0, q_\parallel) = \eta_B \tag{37}$$

$$\hat{\eta}_1(q_\perp, 0) = \eta_S \tag{38}$$

$$\hat{\eta}_2(q_\perp, 0) = \eta_T \,. \tag{39}$$

Experimental arrangements were used to permit evaluation of τ_1 and τ_2 with either $q_\perp$ and $q_\parallel$ equal to zero, with the results shown in Fig. 8 [20].

Values of the Frank free energy constants and the viscosities determined for η_T, etc. are given in Table 2, along with similar data reported [21] for nematic solution of poly(γ-benzyl glutamate) PBG. In computing the free energy constants for PBT, $n_e - n_0$ was calculated from the relation

$$n_e - n_0 = 1.0\ (c/ml.g^{-1}) \tag{40}$$

given elsewhere [1] for a solution of PBT in methane sulfonic acid.

(a) Data for nematic solution of poly(γ-benzyl glutamate) in a mixed solvent (methylene chloride and dioxane) at a concentration just above the isotropic to nematic transition ($w \approx 0.13$) [21].

(b) The solution of PBT in methane sulfonic acid discussed in the text.

(c) The viscosity determined from the steady stress for strain less than unity is entered, see the text.

The data in Table 2 for the PBT and PBG nematic solution are similar in that for both solutions K_1 is smaller than K_B or

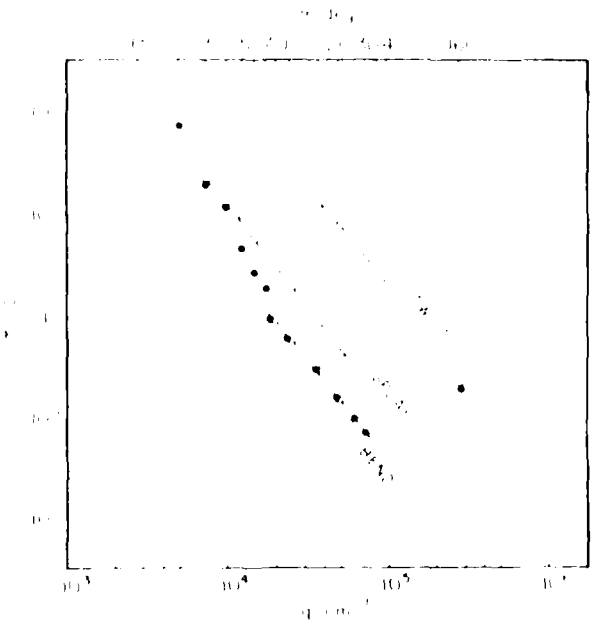

Figure 8. Coherence times as a function of the modulus q of the scattering vector for several optical arrangements: $G^{(2)}_{Hv,\perp}(q_\perp, 0; T), 0$; $G^{(2)}_{Hv,\parallel}(q_\perp, q_\parallel; \tau)$ or $G^{(2)}_{Vh,}(\parallel q_\perp, q_\parallel; \tau)$, •; $G^{(2)}_{Hh,\parallel}(q_\perp, q_\parallel; \tau)$, □; and $G^{(2)}_{Hv,\parallel}(0, q_\parallel; \tau)$, Δ. The lines are drawn with slope -2, indicating the behavior for twist, splay and bend.

K_S. For the PBT solution, K_S is appreciably larger than K_B. These features are in accord with some predictions based on molecular models which predict enhancement of K_S owing to chain-end concentration in splay modes [22]. The values of η_T, etc. in Table 2 give θ_0 equal to 22 deg and 4 deg for the PBT and PBG solutions, respectively. Use of Eq. (20) and the data on Table 2 give the estimate $\alpha_1 = -1.1\eta_T$ for the solution of PBT.

Table 2. Elastic and Viscosity Parameters for Nematic Solutions of Rodlike Polymers

Mode	Parameter	PBG[a] Solution	PBT[b] Solution
Twist	K_2/pN	0.36	1.15
Splay	K_1/pN	4.1	18.2
Bend	K_3/pN	4.7	8.4
Twist	η_T/Pa • s	3.47	220
Splay	η_S/Pa • s	3.45	190
Bend	η_B/Pa • s	0.02	30
	η_0/Pa • s		100[c]

RHEOLOGICAL BEHAVIOR FOR RECENTLY SMALL STRAIN

As illustrated by the data in Fig. 1, frequently for nematic fluids η_κ is found to increase without bound as κ is decreased for small κ. Remarkably, in this range R_κ is independent of κ (*i.e.*, $R_\kappa \approx R_0$). For $\eta_p R_0 \kappa \approx 1$, η_κ is about a constant η_p, independent of κ. For further increase in κ, both η_κ and R_κ decrease with increasing κ. These features are reproducible in that the same η_κ and R_κ are obtained with either increasing or decreasing κ.

The behavior at small κ is similar to that described by Eq. (24) for η_δ as a function of κ, suggesting a nonuniform flow pattern at low κ. The latter could result from the effects of a boundary layer created by adsorbed polymer on the rheometer platens, and the long orientational coherence lengths of the nematic fluid. The light scattering data discussed in the preceding section suggest that an adsorbed layer is important in determining the orientation of the director in the fluid at equilibrium. Although the cone-and-plate geometry has not been analyzed, results on several other geometries [16] suggest that

$E_1 \approx 4\pi^2 h^2 \sigma / K_1$ for torsion between parallel plates with separation h and radius R ($h << R$), and $E_1 \approx 4\pi^2 \sigma R^2 \theta^2 / K_1$ for torsion between cone-and-plate with cone angle π-θ and radius R. For the data illustrated in Fig. 1, $0.1 < (\sigma/\text{Pa}) < 1$ for the range at low κ of interest (*i.e.*, $\eta_p R_0 \kappa < 1$). For the rheometers used, $\theta = 0.035$ radian and R = 2 cm for the cone-and-plate geometry, and h ≈ 0.1 cm and R = 2 cm in parallel plate geometry, so that for the relation given above, $E_1 >$ ca. 10^5 in either case for the range studied with $\eta_p R_0 \kappa > 1$. Calculations for the flow between parallel plates [16] predict that the boundary layer should be small, with minimal effect (*e.g.*, $\eta_\delta \approx \eta_0$) if $E_3 >$ ca. 10^3, however, this depends somewhat on the orientation of the adsorbed layers relative to the flow direction. Nevertheless, it appears that the behavior for the nematic fluid exhibited in Fig. 1 for small κ cannot be explained by application of Eq. (24).

Additional insight to the behavior at small κ is afforded by experiments with a ramp strain (*i.e.*, $\gamma(t) = \kappa t$). In this case one can examine the behavior at small strain for flow with small κ. The sample described in the preceding was investigated in torsional flow with a ramp strain history, *i.e.*, the torsion angle $\phi(t) = \Omega t$. The transmission $T_+(t)$ with crossed polars was obtained as a function of t for several Ω for flow between parallel discs (h = 0.03 cm); the polarizer was oriented at 45 deg. from the flow direction. The sample had a smooth texture at the inception of flow. The stress $\sigma(t)$ was measured for flow between cone-and-plate ($\theta = 0.035$ radians). Following onset of flow, $T_+(t)$ decreased monotonically with increasing t and $\sigma(t)$ rapidly reached a constant value, see Fig. 9. For this flow, $E > 10^5$, so that at steady state the boundary layer would be expected to be very thin, and the measured viscosity may be η_0 given by Eq. (20). With Eq. (21), the data in Table 2 give an orientation angle $\theta_0 \approx 22$ deg. For the polarizer orientation specified,

$$T_+(t) = (1/2)[1 - \cos(4\beta(t))] \sin^2(\delta(t)/2) \qquad (41)$$

where $\beta(t)$ is the angle between the axis of the polarizer and the

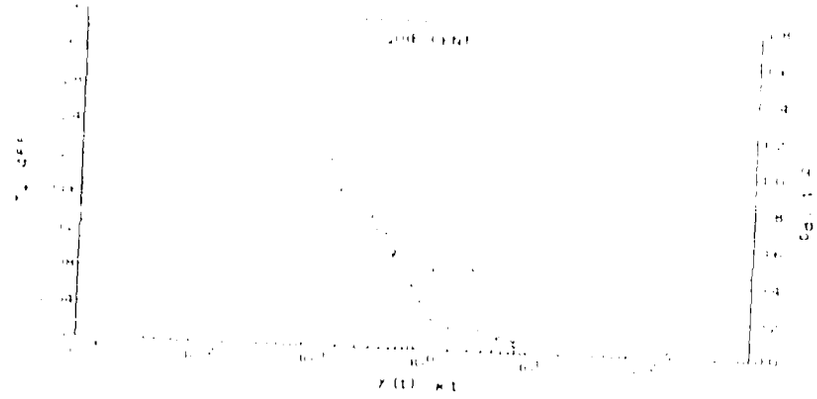

Figure 9. The stress $\sigma(t)$, 0, and transmission $T_+(t)$, $\frac{1}{0}$, as a function of t for deformation at constant stress rate κ for c nematic PBT solution (0.041 weight fraction). The dashed line gives the level of $T_+(t)$ for the quiescent fluid. The polarizer is oriented at 45° from the flow direction in measurement of T_+.

unique axis (n_e) of the refractive index ellipsoid, and the retardation is given by

$$\delta(t) = 2\pi h \Delta n_{13}(t)/\lambda \tag{42}$$

with λ the wavelength of the incident light in a vacuum. Thus, if the rodlike chains are oriented at angle θ_0 to the flow direction in well-developed flow with negligible boundary layer, then instead of using $n_e - n_0$ given by Eq. (40) to compute Δn_{13}, one would use $[n_0^{-2} \sin^2\theta_0 + n_e^{-2} \cos^2\theta_0]^{-1/2} - n_0$ with the result that Δn_{13} is reduced. This may be consistent with the decrease in $T_+(t)$ observed following onset of flow. However, in addition, an extinction cross should be observed. No such extinction cross was observed, indicating that the expected uniform, orientation had not been achieved. (For these experiments the dichroic nature of the nematic PBT fluid is not relevant since the optical

absorption is negligible for the 633 nm wavelength light used). With isotropic solutions of PBT under similar condition [1], an extinction cross is observed along the polarizer and analyzer directions, and the retardation δ increases monotonically with increasing κ until it reaches its limiting value $2\pi h(n_e - n_0)/\lambda$, and $T_+ \propto \sin^2(\delta/2)$. Thus, for isotropic fluids, T_+ increases with increasing κ for small κ.

As the strain γ exceeded about 1 to 2 in the flow with a ramp strain (independent of κ, for small κ), the smooth texture was replaced by a mottled texture, resulting in substantial light scattering, and reduction of both T_+ and $T_\parallel$ to very small values. In addition, the stress was observed to oscillate, finally coming to a new, higher steady-state value. Thus, if the flow for small γ may be interpreted to give η_0, then the final steady state flow gives $\eta_\kappa > \eta_0$. The texture at steady-state flow under these conditions is similar to that obtained if flow is initiated with a mottled texture, such as that realized prior to annealing a newly formed nematic phase (e g , as obtained by cooling an appropriate isotropic solution). The slow reduction in η_κ for small κ shown in Fig. 1 for the nematic fluid corresponds to experiments on such a state. As κ is increased, η_κ tends to reach a plateau value η_p for $\kappa \approx [\eta_p R_0]^{-1}$, with the texture returning to a more smooth appearance. For the solution discussed in the preceding, η_p approximates η_0 given by Eq. (25), but it is not known whether this correspondence is generally obtained. Nevertheless, according to the arguments given, it appears that $\eta_\kappa > \eta_0$ for small κ, so that it is not unreasonable for η_p to be near η_0 in general. However, the preferred orientation θ_κ of the director with the flow direction may be closer to zero than to the orientation θ_0 predicted by Eq. (21) for very slow flow (e g , $\theta_0 = 22$ deg for the PBT solution studied). In that case, η_0 may be about equal to η_b. The observed mottled texture and consequent strong scattering may result from flow instabilities initiated by differences in the angle of adsorbed chains and those in flow as the latter tend toward a preferential orientation. Alternatively, the competition between orientation at the predicted slow flow orientation angle θ_0 and an orientation angle closer to zero for the finite flow velocity may cause the instability.

The recoverable strain $\gamma_R(t)$ has been measured as a function of the time following cessation of steady flow in cone-and-plate rheometry [3]. As shown in Fig. 10, for shear rates such that $\eta_p R_0 \kappa \approx 1$, the data for $\gamma_R(t)/\sigma$ *versus* $t/\eta_p R_0$ are very similar to the corresponding curve for $R_0(t) = \gamma_R(t)/\sigma$ *versus* t/τ_c obtained for the linear viscoelastic behavior of isotropic solutions of PBT (*e g*, a solution with slightly smaller concentration than the nematic fluid). The linear viscoelastic data can be represented in terms of a distribution of retardation times λ_i by the expression

$$R_0 - R_0(t) = \Sigma R_i \exp - t/\lambda_i \ . \tag{43}$$

The similarity of the reduced curves in Fig. 10 indicates that the spread of the distribution of the reduced retardation times, λ_i/τ_N and λ_i/τ_c for the nematic and isotropic fluids, respectively, are similar, where for the nematic fluid,

$$\tau_N = \eta_p R_0 \tag{44}$$

plays the role of τ_c for the isotropic fluid.

The appearance of a recoverable strain following cessation of steady-flow of a nematic fluid is not unique to solutions of PBT (or PPTA). For example, as shown in Fig. 11, such behavior is also observed with a nematic solution of poly (γ-benzyl glutamate), PGB [23,24]. In this case measurements [23] of $N_\kappa^{(1)}$ revealed ranges of κ for which $N_\kappa^{(1)} < 0$; by contrast, $R_\kappa > 0$ for all κ. The appearance of negative $N_\kappa^{(1)}$ has been predicted for nematic fluids (for flow with recently small strain), dependent on the viscosity coefficients α_i and the preferred orientation of an adsorbed layer [25]. For the data shown in Fig. 11, κ is probably too large to give the true slow flow behavior, but perhaps the general feature predicted for $N_\kappa^{(1)}$ may be valid if the preferred direction θ_0 in slow flow is replaced by a preferred direction θ_κ which decreases toward zero with increasing κ. In this case, the dependence of $N_\kappa^{(1)}$ on κ would be attributed to the coupling of θ_κ with the preferred orientation at the boundary. According to

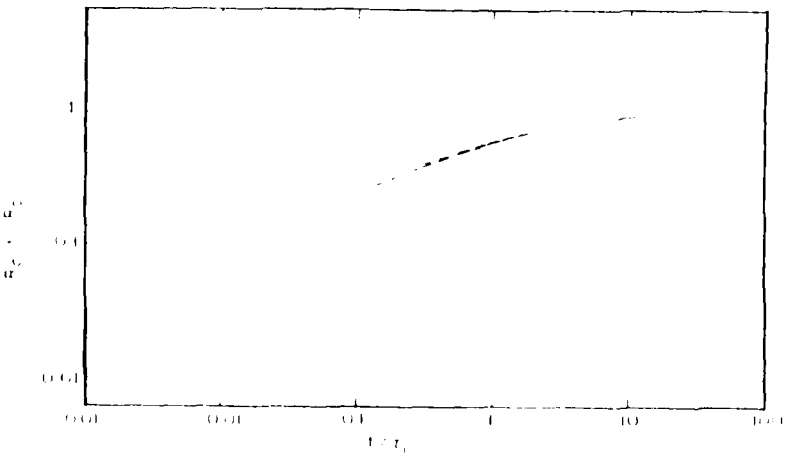

Figure 10. $R_0(t)/R_0$ *versus* τ/T (with $\tau_c = \eta_0 R_0$) for an isotropic solution of PBT (0.0294 weight fraction polymer), ---, and $R_\sigma(t)/R_\kappa$ *versus* $t/\eta_p R_\kappa$ for a nematic solution of the same polymer (0.0323 weight fraction polymer), _____. For the latter, $R_\sigma(t)$, R_κ and η_p were determined after steady-state flow with $\eta_p R_\kappa \kappa \approx 1$. (From reference 3).

a treatment of Currie [25] based on the Leslie-Ericksen constitutive equation, for flow between parallel plates with recently small strain,

$$\nu^{(1)}/\sigma \propto \sin\theta_{AD} \cos\theta_{AD} [\alpha_1 + \eta_T/\cos 2\theta_0] \tag{45}$$

where θ_{AD} is the orientation of the adsorbed layer with respect to the flow direction. Since $\alpha_1 < 0$, this relation can give $N_\kappa^{(1)} < 0$. If Eq. (45) is approximately valid for flow at larger κ, merely by replacement of θ_0 by θ_κ, then it would be possible to transform from conditions with $N_\kappa^{(1)} > 0$ to $N_\kappa^{(1)} < 0$ as θ_κ decreased toward zero with increasing κ.

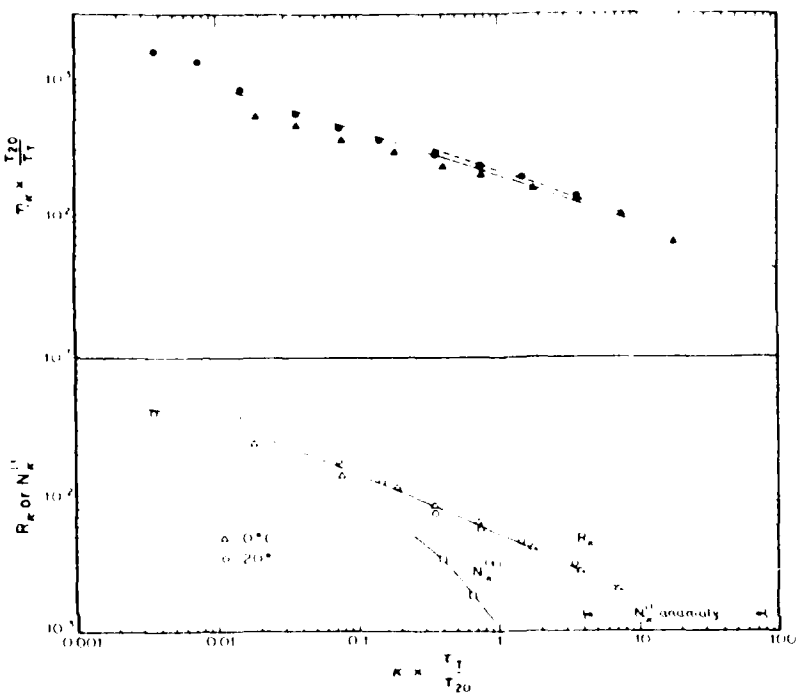

Figure 11. $\eta_\kappa(\tau_{20}/\tau_T)$. R_κ and $N_\kappa{}^{(1)}$ *versus* $(\tau_T/\tau_{20})\kappa$ for an anisotropic solution of poly(γ-benzylglutamate) in cresol for T/K equal to 273 (Δ, Δ) and 293 (0,°). The dashed line and the data on N_κ are from reference 23. The factor τ_T/τ_{20} is unity for T = 293K and chosen to superpose data on R_κ *versus* $(\tau_T/\tau_{20})^\kappa$ for T = 273K. The range denoted "$N_\kappa{}^{(1)}$ anomaly" designates the range for negative $N^{(1)}{}_\kappa$ according to reference 23. (From reference 3).

RHEOLOGICAL BEHAVIOR FOR LARGER STRAIN RATES

As κ is increased so that $\tau_N\kappa > 1$, the optical appearance becomes more like that of a isotropic rodlike solution in flow with $\tau_c\kappa > 1$. The birefringence increases, but unlike the behavior with isotropic fluids, large fluctuations of Δn_{13} during flow restrict measurements of T_+, see below. The stress is easily measured, without noticeable fluctuations.

The functions η_κ and R_κ both decrease with increasing κ for $\tau_N\kappa > 1$. Consistent with the optical data, the decreasing η_κ for $\eta_\kappa < \eta_p$ may be attributed to progressive increase in the local order parameter S, and with flow orientation angle θ_κ nearly zero, under the influence of flow with $\kappa > \tau_N^{-1}$. Thus, in the first approximation, one might approximate η_κ by use of Eq. (24-25), with S an (unknown) function of κ. In this flow regime the isotropic and nematic fluids exhibit similar flow curves (*i.e.*, η_κ/η_0 *versus* $\tau_c\kappa$ for the isotropic fluid or η_κ/η_p *versus* $\tau_N\kappa$ for the nematic fluid), despite the dissimilarities in the magnitudes of η_0 and η_p or the R_0. Consequently, Eq. (5) is a useful representation for η_κ/η_p *versus* $\tau_N\kappa$, and, for the PBT fluids studied, the properly normalized distribution of relaxation times obtained for the isotropic fluid may also be used for the nematic fluid of comparable M_w (*e.g.*, τ_i/τ_c in the distribution for the isotropic is replaced by τ_i/τ_N to obtain the distribution for the nematic).

During steady flow, T_+ and $T_\parallel$ (measured with the polarizer at angle $\pi/4$ from the flow direction) are nearly equal, and tend to undergo nearly periodic fluctuations, with a mean that increases with κ-- these fluctuations are not obtained with isotropic solutions of PBT for flow with $\tau_c\kappa$ comparable to $\tau_N\kappa$.

The fluctuations in T_+ and $T_\parallel$ may be related to the appearance of the nonbirefringent bands noted above in the preparation of the monodomain of a PBT solution. According to a treatment by Marrucci [26] based on the Leslie-Ericksen constitutive equation, the unstable shear flow will be manifested as a periodic rotation of the director orientation between angle θ_0 and $-\theta_0$, with the period T of the oscillation being equal to $\pi(|\alpha_2|/\alpha_3)^{1/2}/\kappa$ if $\alpha_3 << |\alpha_2|$. Such an effect would give rise to the observed behavior, but would not be expected for PBT

solution if α_3 and α_2 have the values found from the light scattering studies since the latter lead to stable shear flow. The unstable flow might correspond to the predicted behavior using the values of α_2 and α_3 modified by the strong shear flow. In some cases, on cessation of flow, T_+ increases to a very large value for a short time (ca. $\tau_N/100$) before decreasing to a very low value, nearly equal to the transmission for a isotropic state. Subsequently, T_+ increases slowly, in all cases eventually reaching a value near the initial value. The fluctuation in T_+ during flow and the behavior during relaxation on cessation of flow both indicate that the molecular alignment in flow may not be a simple uniaxial orientation at some angle θ_κ relative to the flow direction. The dependence of T_+ on time at long time following cessation of flow is probably controlled principally by the return of the director field to the planar, twisted orientation obtained in the equilibrium quiescent fluid owing to the effects of the adsorbed layer of polymer. The small values of T_+ and $T_\parallel$ observed for shorter time on cessation of flow could result from a texture with oscillations in the director orientation as a function of the position along the perpendicular to the surfaces (there could even be complete rotation of the director orientation). Thus, the sharp increase in T_+ with subsequent marked drop could be caused by momentary alignment of the optic axis along the former flow direction as the optic axis at each plane recoils from its direction in flow to a new direction in response to the viscoelastic memory of the fluid. Subsequently, this nonequilibrium texture gradually relaxes to the equilibrium texture prescribed by the orientation of chains adsorbed on the surfaces.

Following cessation of steady flow, the recoverable strain reaches its final value γ_R at a time for which T_+ remains low. Consequently, quantitative explanation of the behavior for R_κ may be expected to be complex. The inherent time scale of the recovery is of order τ_N, but for example, the dependence of R_κ/R_0 on $\tau_N\kappa$ cannot be represented by Eq. (6). Neither is it known what relation might exist between R_κ and $N_\kappa^{(1)}$.

The effects described in the preceding have obvious application in solution processing of nematic polymeric fluids to give preferred direction to the molecular chains. Both more systematic experiments and improved theoretical insights are needed to advance our understanding of the rheological behavior and our ability to manipulate the preferred direction of the nematic fluid with an applied stress. In particular, a constitutive equation is needed for a polymeric nematic fluid that includes memory effects, and questions of flow stability need further elucidation.

ACKNOWLEDGEMENT

This work described above was carried out under partial support from the Polymers Program, Division of Material Research, National Science Foundation, and the Materials Laboratory, Wright-Patterson Air Force Base. Certain of the rheological measurements were obtained by Mr. C. S. Kim.

REFERENCES

1. S.-G. Chu, S. Venkatraman, G. C. Berry and Y. Einaga, Macromolecules 14, 939 (1981).
2. S. Venkatraman, G. C. Berry and Y. Einaga, J. Polym. Sci., Polym. Phys. Ed. 23, 1275-1295 (1985).
3. Y. Einaga, G. C. Berry and S.-G. Chu, Polymer J. 17, 239 (1985).
4. L. J. Zappas and J. C. Phillips, J. Res. Natl. Bur. Stand, Sec. A 75A, 33 (1971).
5. M. Doi and S. F. Edwards, J. Chem. Soc. Faraday Trans 2 74, 560 (1978).
6. J. D. Ferry, Viscoelastic Properties of Polymers, 3rd. ed., Wiley, New York (1980).
7. K. Nakamura, C.-P. Wong and G. C. Berry, J. Polym. Sci., Polym. Phys. Ed. 22, 1119 (1984).
8. M. Doi, J. Phys. (Paris) 36, 607 (1975).
9. F. M. Leslie, Adv. Liq. Cryst. 4, 1 (1979).
10. M. Miesowicz, Nature 158, 27 (1946).

11. O. Parodi, J. Phys. (Paris) 31, 581 (1970).
12. J. P. van der Meulen and R. J. J. Zijlstra, J. Physique 45, 1627 (1984).
13. P. G. deGennes, The Physics of Liquid Crystal, Clarendon Press, Oxford (1974).
14. S. Chandrasekhar, Liquid Crystals, Cambridge University Press, Cambridge (1977).
15. N. Kuzuu and M. Doi, J. Phys. Soc., Jpn. 53, 1031 (1984).
16. P. K. Currie and G. P. Mac Sithigh, J. Mech. Appl. Math 32, 499 (1979).
17. N. Kuzuu and M. Doi, J. Phys. Soc. Jpn 52, 3489 (1983).
18. G. Marrucci, Mol. Cryst. Liq. Cryst. (Lett.) 72, 153 (1982).
19. P. J. Flory, Proc. R. Soc. (London) Ser. A 234, 73 (1956).
20. K. Se and G. C. Berry, to be published.
21. V. G. Taratuta, A. J. Hurd and R. B. Meyer, Phys. Rev. Lett. 55, 246 (1985).
22. R. B. Meyer in Polymer Liquid Crystals, ed. by A. Ciferri, W. R. Krigbaum and R. B. Meyer, Academic, New York, 1982.
23. G. Kiss and R. S. Porter, J. Polym. Sci., Polym. Sym. 56, 193 (1978).
24. G. C. Berry, Discussions Faraday Soc. No. 79, 141 (1985).
25. P. K. Currie, Mol. Cryst. Liq. Cryst. Liq. Cryst. 73, 1 (1981).
26. G. Marrucci, Pure and Appl. Chem. 57, 1545 (1985).